AGU PUBLICATIONS

Geophysical Research Letters

RESEARCH LETTER
10.1002/2015GL064030

Key Points:
- Satellite data show impact of soil moisture on convective initiation in Europe
- Initiation occurs preferentially on soil moisture gradients
- Processes important in semiarid tropics also affect Europe

Correspondence to:
C. M. Taylor,
cmt@ceh.ac.uk

Citation:
Taylor, C. M. (2015), Detecting soil moisture impacts on convective initiation in Europe, *Geophys. Res. Lett.*, *42*, 4631–4638, doi:10.1002/2015GL064030.

Received 27 MAR 2015
Accepted 12 MAY 2015
Accepted article online 14 MAY 2015
Published online 3 JUN 2015

Detecting soil moisture impacts on convective initiation in Europe

Christopher M. Taylor[1,2]

[1]Centre for Ecology and Hydrology, Wallingford, UK, [2]National Centre for Earth Observation, Wallingford, UK

Abstract Feedbacks between soil moisture and precipitation are important for understanding hydroclimatic variability in many regions. However, much uncertainty remains about how land surface fluxes influence the initiation of deep convection locally. While some studies consider only atmospheric and soil profiles, in a one-dimensional sense, others have argued that horizontal variability in fluxes plays an important role in convective triggering, via mesoscale circulations. This paper presents the first comprehensive observational analysis over Europe linking convective initiation to soil moisture, based on satellite observations of cloud top and land surface temperature, and soil moisture. The results show that convective initiations are favored on the downwind side of dry surfaces, close to wetter areas. The signal is clearest following dry periods and under light winds, consistent with forcing by a mesoscale circulation. Overall, the detected signal in Europe is weaker than in previous Sahelian analysis, but key spatial characteristics are essentially the same.

1. Introduction

Soil moisture can influence rainfall by limiting evapotranspiration, which affects the development of the daytime planetary boundary layer (PBL) and thereby the initiation and intensity of convective precipitation [e.g., *Eltahir*, 1998]. Feedbacks between soil moisture and precipitation are considered important in many regions for weather prediction [*Koster et al.*, 2004] and regional hydroclimatic variability. Under future climate scenarios, with higher evaporative demand driving increased soil moisture deficits in many places, soil moisture-precipitation feedbacks may play an increasingly important role [*Dirmeyer et al.*, 2013; *Seneviratne et al.*, 2013].

One key aspect in the feedback loop is the impact that soil moisture has on the local initiation of moist convection. A number of authors have analyzed this impact using simple one-dimensional models of the surface and PBL [*Ek and Holtslag*, 2004; *Findell and Eltahir*, 2003], and found that the sensitivity of moist convective initiation to soil moisture depends on the vertical profile of the atmosphere. Another branch of the literature has focused on the role of mesoscale variations in soil moisture (and vegetation) in the development of daytime PBL circulations, which provide a favorable environment for the triggering of deep convection [*Avissar and Liu*, 1996; *Pielke*, 2001]. The importance of the latter (2-D) land surface effects over the former (1-D) effects has been demonstrated from high-resolution observations in both the moist [*Knox et al.*, 2011] and semiarid tropics [*Taylor et al.*, 2011, hereafter T11]. These observational findings are important as much of the numerical modeling work on feedbacks in previous decades relied on coarse resolution simulations employing basic parameterizations of convection. These parameterizations have been shown to be unreliable compared to convection-permitting simulations [*Hohenegger et al.*, 2009]. Indeed, a recent global study [*Taylor et al.*, 2012, hereafter T12] showed that while afternoon rain is observed more frequently over drier soils relative to nearby (50–100 km) wetter areas, global atmospheric models reliant on convective parameterizations consistently simulate more frequent rain over wetter soils. While the spatial resolution of the global models is one factor, subsequent work using several configurations of a single model [*Taylor et al.*, 2013] has shown that it is the convective parameterization which results in a strong positive feedback between soil moisture and precipitation.

The importance of soil moisture for the initiation of deep convection varies regionally, depending on both the sensitivity of evapotranspiration to soil moisture and the sensitivity of the atmosphere to surface flux forcing [*Guo et al.*, 2006]. In the midlatitudes, feedback studies have tended to focus on the United States, and the Great Plains in particular [*Koster et al.*, 2003], where variations in soil moisture deficit provide some medium-range predictability, at least for temperature [*Koster et al.*, 2010]. There have been relatively few papers examining the impact of soil moisture on rainfall in Europe, in part because the signal is likely

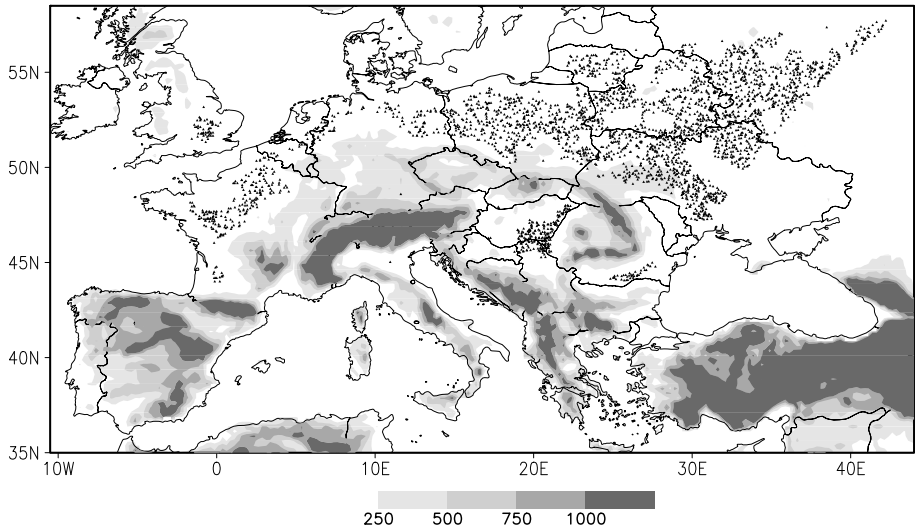

Figure 1. Topographic height (m) across the study area, plotted at a resolution of 0.25° for clarity. The location of each initiation is denoted by a triangle.

weaker [*van den Hurk et al*., 2012]. Several studies have explored surface coupling with convection in the Netherlands using a one-dimensional coupled surface boundary layer model [*Ek and Holtslag*, 2004; *van Heerwaarden et al*., 2010], while *Boé* [2013] examined statistical relationships between rainfall, soil moisture, and circulation types across regions of France. *Schär et al*. [1999] simulated a positive soil moisture-precipitation feedback within a regional climate simulation and identified the importance of boundary layer processes in triggering convection on this feedback. However, as noted above, when this issue was revisited using a convection-permitting simulation over Central Europe, *Hohenegger et al*. [2009] found that its more realistic depiction of convection resulted in a negative rather than positive feedback. At the same time, several papers [e.g., *Hauck et al*., 2011] have examined the impact of realistic soil moisture initialization on simulated convective rain in complex terrain and found strong, but situation-specific, precipitation responses.

This paper uses satellite observations to analyze for the first time the land surface environment in which convective initiations develop across Europe. A similar approach to the Sahelian study of T11 is adopted, whereby a large data set of convective initiations is constructed using cloud top temperatures. Statistically robust relationships with preinitiation land surface temperature (LST) and soil moisture patterns are identified, which shed light on the relative importance of 1-D and 2-D mechanisms in Europe. This complements the previous global study (T12) which focused on afternoon rain (not just initiation) and, because of the resolution of the data, could not distinguish between 1-D and 2-D processes. The role of wind conditions on the feedback as discussed by *Froidevaux et al*. [2014] is also considered. The paper proceeds with a description of the observational data sets and methods (section 2), and is followed in section 3 by the results and concludes with a discussion of the differences between processes dominating in Europe and the Sahel.

2. Data and Methods

An observed data set of deep convective initiations is constructed from cloud top temperature data (10.8 μm) obtained every 15 min by the Spinning Enhanced Visible and Infrared Imager, on board the Meteosat Second Generation series of geostationary satellites. Pixel size varies between 13 km^2 in south-western Europe to 59 km^2 in the far north-east (Figure 1). Images between 1100 and 1745 UTC are analyzed for each month from April to September for the years 2004–2013.

Convective initiations are identified from rapidly cooling cloud top temperatures [e.g., *Morel and Senesi*, 2002]. Specifically, all appearances of a new local minimum pixel temperature T_{min} colder than some threshold (here set to −35°C) are identified. To minimize the number of false "initiations" due to either propagating cold cloud or modest decreases in cloud top temperature from a stationary cloudy area, an

additional criterion must be satisfied for nearby pixels in the preceding hour. For each of these four images, if the minimum temperature within a radius (set to 30 km) corresponds to a rate of $dT_{min}/dt > -10$ K/h, then the case is rejected.

For this study, it is important to filter out initiations potentially associated with strong orographic, coastal, and lake triggers. Initiations are therefore also rejected if they occur within 50 km of sea points, inland water bodies greater than 9 km^{-2}, or topographic height variations within 50 km exceeding 250 m. These somewhat arbitrary thresholds are chosen to yield enough initiations to produce robust statistics while minimizing the impact of topographic features on the analysis. Water bodies are defined from the Moderate Resolution Imaging Spectroradiometer (MODIS) land cover classification at 500 m and topographic variability computed from the GTOPO30 data set (https://lta.cr.usgs.gov/GTOPO30) at 30 arc s resolution (~1 km). Following filtering, a total of 2962 initiations are retained, located predominantly across Eastern Europe (Figure 1). With the exception of 10 initiations in northern Spain, the entire Mediterranean portion of the domain is excluded due to either topography or coastal filtering. Considering that the entire land area sampled in this study (i.e., noncoastal and flat) is close to 1,000,000 km^2, the initiation data set corresponds to an average of approximately three initiations per year per 100 km × 100 km box.

To characterize land surface properties in the vicinity of each initiation, a combination of complementary data sets are used. The primary data source is land surface temperature (LST). Temporal LST anomalies (LSTAs) can provide a useful proxy for soil moisture if air temperature variations are accounted for. This study focuses on snapshots of mesoscale LSTA structures, where gradients in air temperature are expected to be small and are in part responding to soil moisture anomalies. Locally positive LSTAs are indicative of positive sensible heat flux anomalies relative to the surroundings, an approach exploited by T11 to map Sahelian soil moisture patterns in the vicinity of convective initiations. In this study, LSTA data are derived from MODIS measurements on the Terra satellite. The daily level 1 collection 5 version of the data set (MOD11A) is used, corresponding to a resolution of 1 km and a typical morning overpass time of 1100 LT. Only cloud-free data satisfying the highest level quality control flag of 0 (see https://lpdaac.usgs.gov/products/modis_products_table/mod11a1) are used, with quoted average LST errors up to 1°C. This excludes most urban areas. In addition, only view angles of less than ±55° are retained. A monthly mean LST climatology is constructed for the period 2000–2013 on the 1 km grid from which daily LSTAs are computed.

Compared to semiarid regions, the use of LSTA to infer surface flux behavior is more challenging in densely vegetated and wetter climates. However, their utility has been demonstrated in a variety of European studies for monitoring soil moisture and associated surface flux anomalies [*Zaitchik et al.*, 2006]. The application of LST here is evaluated using independent surface soil moisture index measurements from the advanced scatterometer (ASCAT) instrument [*Bartalis et al.*, 2007], available typically daily (either 1030 or 2230 LT) from 2007 onward, containing information on soil moisture in the top few centimeters on scales ~25 km. Anomalies in soil moisture on the native grid of 12.5 km are computed relative to the 7 year monthly climatology, and pixels containing water bodies, complex topography, frozen soil are removed. Following T12, pixels where day-to-day changes in soil moisture are not positively correlated with rainfall at the 95% level are also excluded.

Following the approach of T11, LSTA and soil moisture are computed as a function of location (±100 km) relative to each initiation, having first oriented the fields in the direction of the large-scale low-level flow. The wind information is taken from the 10 m components at 12 UTC at the closest grid point in the ERA-Interim reanalysis [*Dee et al.*, 2011]. The individual cases are averaged to produce composite mean surface fields relative to the initiation. Care is required to minimize the indirect influence of cloud on the composite LSTA field. First, only events with valid (cloud-free) LST data covering at least 25% of the 200 × 200 km area are retained. Then the 1 km data are aggregated up to 5 × 5 km boxes, and boxes with less than 50% cloud-free cover are excluded. Taken together, these measures ensure that the 1 km data represent conditions within larger cloud-free areas. To minimize similar sampling issues with the soil moisture data, only cases with at least 75% valid ASCAT pixels go forward for the analysis. Note that the overall results presented are rather insensitive to the choice of thresholds set out above.

3. Results

The mean two-dimensional structure of LSTA is presented in Figure 2, based on the average of midmorning Terra data on the day of the event or, in cases of substantial cloud and/or no local overpass, the preceding

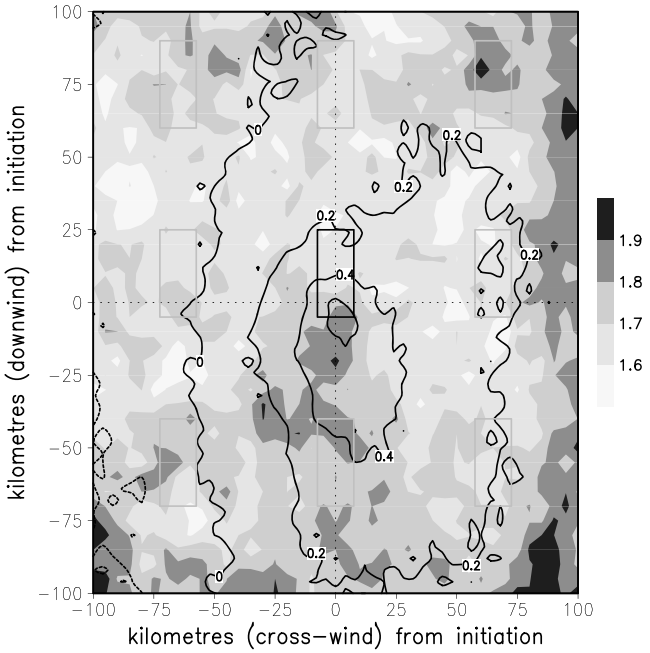

Figure 2. Composite mean LSTA (shaded; K) from 1544 convective initiations over Europe. For each event, the LSTA data were regridded relative to the initiation point (defined at 0,0) according to the low-level large-scale midday wind direction (wind flowing from bottom to top). The contours denote LSTA from T11 based on 3765 Sahelian initiations. The rectangles denote the locations used to compute LSTA gradients for the initiation (black) and noninitiation (gray) samples.

day. Note that similar (though noisier) patterns are found when treating the two days individually. The composite depicts positive LSTA everywhere, but with relatively warm conditions over and upwind of the initiation point, and around much of the edge of the 200×200 km domain. While the overall field is certainly noisy, the pattern of locally warmer conditions around the initiation point appears similar, in orientation, extent, and upwind offset, to the elliptical LSTA structure presented by T11 (and reproduced in Figure 2) for the Sahel. In the Sahel case, the central pattern is more clearly defined and of larger amplitude than in this study. Also note that in the Sahel analysis, the plotted field has already had a domain average LSTA removed, resulting in smaller absolute values.

Replicating the methodology of T11, for each event, downwind LSTA gradients were computed over a distance of 30 km, centered on a location 10 km downwind of the initiation point (black rectangle in Figure 2). Alongside this "initiation" sample of $n_i = 787$ cases with sufficient local LST data, a "noninitiation" sample of $n_{ni} = 6058$ LSTA gradients was created using the same days, but where the gradients were computed at eight nearby locations (gray rectangles in Figure 2). The mean initiation gradient of -0.0058 K km^{-1} compared with a mean noninitiation gradient of $+0.0001$ K km^{-1}. Again following T11, to estimate the likelihood that the difference in mean gradients between initiation and noninitiation samples occurred by chance, random combinations of n_i and n_{ni} gradients were drawn without replacement from the pooled sample, and their respective means found. Repeating this process 100,000 times, the difference between initiation and noninitiation gradients was found to be highly significant (p value of 0.0018). Thus, as in the Sahel, convective initiation in Europe occurs preferentially over negative LSTA gradients.

To investigate the sensitivity of the above results to soil wetness conditions, the initiation data set was stratified into quartiles of antecedent 30 day rainfall (Figures 3a–3d) using the daily 0.5° gridded gauge data set of *Haylock et al*. [2008]. To provide a basic indication of regional soil water stress, rainfall totals were averaged over a region $2.5 \times 2.5°$, centered on the initiation. Consistent with expectations of a drier surface being warmer, transect mean LSTA increased with decreasing rain in the previous 30 days, ranging from +0.25 K for initiations in the wettest quartile (Q4) to +3.0 K for the driest quartile (Q1). Of more interest here is the spatial variability in LSTA around the initiation point. The negative along-wind LSTA gradient was clearest for Q1, and to a lesser extent for Q2 and Q3. By contrast with the three drier quartiles, the mean gradient in Q4 did not differ significantly from zero at the 90% level.

The physical interpretation of LSTA as a surface energy balance response to soil moisture anomalies was confirmed using surface soil moisture anomalies from ASCAT. In each of the four composites in Figure 3, there is a tendency for mesoscale soil moisture gradients to be anticorrelated with LSTA gradients, though the signal is not evident in all locations. This is perhaps not surprising given the contrasting spatial resolutions of the input data sets (1 km for LST and 25 km for soil moisture) and different subsets of events for which the two data sets are available. However, comparing gradients in anomalies of LST

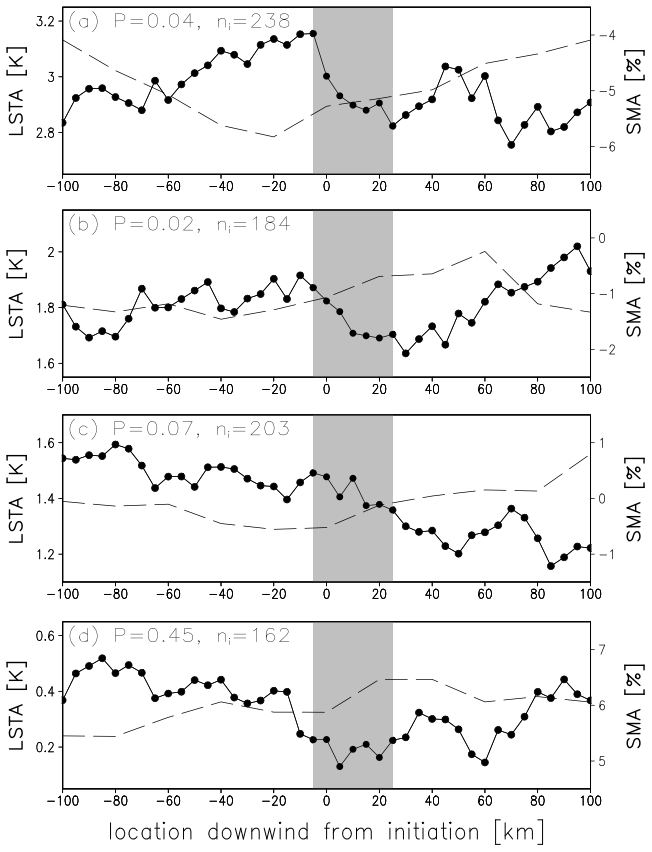

Figure 3. Composite mean LSTA (K; solid line) and soil moisture index anomaly, SMA (%; dashed line) as a function of downwind distance from the initiation, stratified into quartiles according to rainfall R in the previous month. (a) Q1, $R < 35$ mm, (b) Q2, $35 < R < 53$ mm, (c) Q3, $53 < R < 78$ mm, and (d) Q4, $R > 78$ mm. The shading denotes the 30 km zone over which gradients were computed. P values are provided for each quantile based on n_i cases, using the resampling methodology described in the text.

and soil moisture between −5 and +25 km for the 299 events in common, a linear regression was retrieved with a slope of $-0.08\,\mathrm{K\%^{-1}}$, ($P = 0.001$), corresponding to an LST decrease of 8 K between a completely dry and completely wet surface.

The composite mean structure in Figure 2 can therefore be interpreted as the preferential initiation of deep convection in locations with positive along-wind soil moisture gradients, as in the Sahel, with contributions coming from initiations in areas which have received less than 78 mm rainfall in the previous month. The sensitivity to antecedent rain is consistent with a higher sensitivity of fluxes (and therefore convection) to soil moisture when soils are relatively dry, as found by T12. The finding in that study of preferential rain over locally drier soils in Europe thus arises from at least two-dimensional considerations rather than a one-dimensional view [e.g., *Ek and Holtslag*, 2004]. If the latter effect were dominant in producing rain over drier soil, one would expect a positive composite LSTA feature centered on the initiation point or possibly shifted downwind if advection were important.

The spatial structure of the composite LSTA signal is consistent with surface-induced mesoscale convergence zones [*Froidevaux et al.*, 2014; *Pielke*, 2001; *Taylor et al.*, 2013]. Further evidence for a circulation is provided in Figure 4a, which shows the percentage of cloud-free 1 km LST pixels on the preceding day, as a function of along-wind distance from the initiation, excluding events in the wettest quartile (Q4, $R > 78$ mm). In the locally warm zone stretching 25 km upwind of the initiation point, there is a reduction in cloud-free pixels relative to the adjacent areas. This difference, which amounts to ~5% of the mean cover value, is evident neither in the climatology nor initiations in the wettest quartile and is consistent with local variations in shallow cumulus associated with a soil moisture-induced mesoscale circulation on the preceding day.

Finally, to assess the impact of wind speed on the results, the initiation data set is split into high ($>3\,\mathrm{m\,s^{-1}}$) and low ($<3\,\mathrm{m\,s^{-1}}$) wind cases. As discussed by *Froidevaux et al.* [2014], once initiated over a dry-wet soil boundary and given moderate to strong winds, the convection will move downwind, that is over a wetter surface. Cold cloud cover (using a threshold of −40°C) is used in Figure 4b as a proxy for the location of rainfall 1 h after initiation. As expected, the propagation of the cloud distribution downwind is sensitive to wind speed, with a maximum at +20 km (or $5.6\,\mathrm{m\,s^{-1}}$) for high wind cases, and between 0 and 10 km for low-wind cases. Interestingly, for the lightest winds ($<1.5\,\mathrm{m\,s^{-1}}$, not shown), the cloud distribution actually shifts slightly upwind from 0 km. Another aspect to be considered here is the influence of wind speed on the development of soil moisture-induced mesoscale circulations; strong winds reduce horizontal gradients in PBL temperature which drive the circulations, thus potentially suppressing their impact on

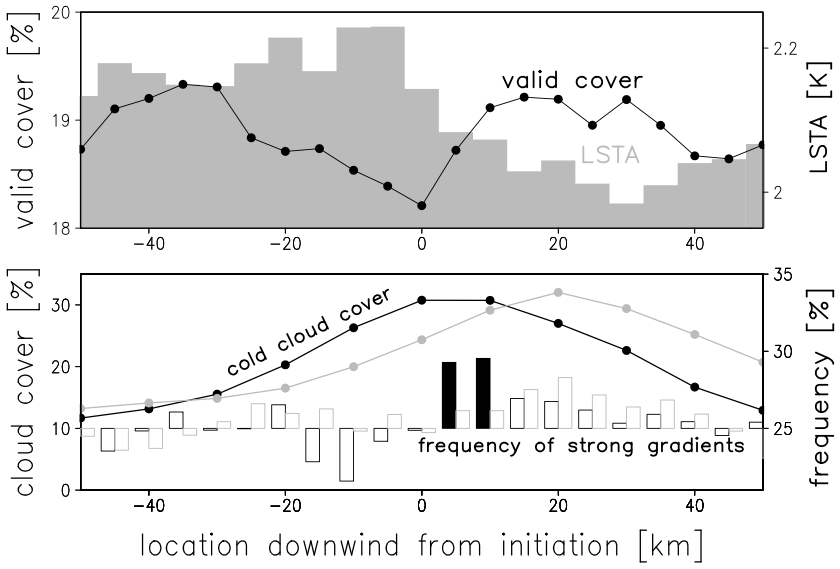

Figure 4. (a) Clear-sky coverage (%; line) on the day preceding initiation, as a function of distance downwind from the initiation. Shading: mean LSTA (K). (b) Cold cloud cover (%; threshold of −40°C) 1 h after initiation, split into high (>3 m s^{-1}; gray) and low (<3 m s^{-1}; black) wind cases. The gray and black bars in these two samples denote the frequency of a strong downwind gradient in LST, where a strong gradient is defined as being within the first quartile. The bars are shaded where strong gradients occur more frequently than expected (i.e., 25% of the time) at the 95% significance level. Note that in Figure 4a, initiations in Q4 have been excluded.

convective initiation. To assess whether this effect is evident in the observations here, Figure 4b also includes the frequency of "strong" negative LSTA gradients observed relative to the initiation locations. For each initiation, a strong gradient is defined as being in the first quartile of all observed gradients on that day within 100 km. This measure was chosen as, unlike mean LSTA, it is independent of wind speed differences between the two sets of events. For the low-wind cases, strong negative LSTA gradients are most often found 5 to 10 km downwind of initiation, and their enhanced frequency here is significant at the 95% level. In the high wind sample however, there is no clear relationship with local LSTA gradients. Qualitatively similar results are found when using ERA-Interim wind data from the 850 hPa pressure level rather than 10 m. While the relationships between surface flux variations (amplitude and length scale), wind speed, and where it actually rains are complex [*Rieck et al.*, 2014], these observations suggest that the surface heterogeneity influence on rainfall in Europe is stronger under lighter winds. One can speculate that this might limit the influence of propagation (highlighted by *Froidevaux et al.* [2014]) on where rain preferentially falls, as soil moisture has a relatively weak impact on initiations under strong winds.

4. Summary and Discussion

This study provides the first observational analysis of soil moisture impacts on convective initiation in Europe. Using a combination of surface and atmospheric data sets, the results reveal strong similarities with previous analysis from semiarid West Africa. Convective initiations are favored on the downwind side of dry surfaces, close to wetter areas. This location is consistent with forcing by a mesoscale circulation induced by differential surface heating. However, there are three factors which contribute to a weakening of the observed signal in Europe compared to the Sahel.

First, evapotranspiration in central and northern Europe is less sensitive to soil moisture than in semiarid regions. In well-vegetated midlatitude regions, strong soil moisture-induced flux heterogeneity will only emerge during lengthy dry spells, when root zone soil moisture deficits start to restrict transpiration. By contrast in semiarid regions where evaporation direct from the soil plays a more important role on the surface energy balance, frequent convective rain events falling on predominantly water-stressed soils create surface fluxes which are highly variable in space and time. In combination with weaker solar forcing, this

means that sensible heat flux heterogeneity on scales ~10–40 km is more modest in Europe. This effect manifests itself in the observed weakening of the mean negative LSTA gradient with increasing antecedent rainfall (Figure 3), such that no surface effect is evident following monthly rain exceeding 78 mm (Q4). In the Sahel by contrast, even at the August peak of the wet season (when rain typically exceeds 100–200 mm month^{-1}, depending on latitude), a strong LSTA gradient signal was evident in the initiations identified by T11. Further comparison between the European and Sahelian analyses can be made by computing the number of initiations over a "strong" negative LSTA gradient (defined as the first quartile of gradients in a noninitiation sample). For the European study, 28.2% of all initiations fall into this category, compared to an expected value of 25% assuming no effect. While this percentage rose with decreasing antecedent rainfall (to 30.7% for cases where monthly rain was in the first quartile), it is markedly lower than the comparable value of 37% for all wet season initiations in the Sahel.

Second, stronger winds in midlatitudes likely suppress the development of daytime mesoscale circulations relative to the Sahel, particularly when surface flux variability is weak. In unpublished analysis of the T11 data set, no wind speed sensitivity was found, unlike here (Figure 4b). When strong soil moisture heterogeneity occurs on a length scale capable of triggering convection under moderate to strong winds typical of central and northern Europe, the rainy system will likely move downwind [*Froidevaux et al.*, 2014]. This situation contrasts with the Sahel, where convection propagates with the midlevel easterly jet, counter to the low-level southwesterly flow. Such wind effects may also contribute to the relative strengths of the two regions in terms of the preference for afternoon rainfall over drier soil on scales of 50 km observed by T12.

Finally, in terms of signal detection, Europe provides more challenging conditions than the Sahel. This study analyzed only ~50 initiations per month, compared to ~190 per month in T11 over a smaller area. The difference arises partly from the use of a conservative filter to exclude regions where topographic and coastal effects may be important; in the case of Europe this represents a considerable fraction of the land area. It also reflects the climatology of the two regions. The Sahelian wet season is characterized by frequent afternoon convective initiations, while rainfall in Europe is often frontal in nature. As noted by other studies [*Koster et al.*, 2004], the stronger synoptic controls on rain in midlatitudes, alongside weaker soil moisture controls on surface fluxes, mean that the climatic impacts of soil moisture-precipitation coupling in central and Northern Europe are less important than in the semiarid tropics. It should be remembered that while this study has examined relationships between soil moisture and convective initiation on scales of tens of kilometers, soil moisture-precipitation feedbacks may also be operating on much larger space scales via both moisture recycling [*van der Ent et al.*, 2010] and surface-induced perturbations to regional circulations [*Fischer et al.*, 2007]. Moreover, by necessity, this study has excluded convective initiations over mountainous regions such as the Alps, which contribute a disproportionately large fraction of summertime storms in Europe.

Acknowledgments

This work was supported by the UK Natural Environment Research Council (NE/I006729/1). The author would like to thank Phil Harris and Rich Ellis for helpful comments on the study, and to Wouter Dorigo for provision of ASCAT soil moisture data. Observational data used in the study can be downloaded from http://archive.eumetsat.int (Meteosat and ASCAT) and http://reverb.echo.nasa.gov/(MODIS).

The Editor thanks two anonymous reviewers for their assistance in evaluating this paper.

References

Avissar, R., and Y. Q. Liu (1996), 3-dimensional numerical study of shallow convective clouds and precipitation induced by land-surface forcing, *J. Geophys. Res.*, *101*, 7499–7518, doi:10.1029/95JD03031.

Bartalis, Z., W. Wagner, V. Naeimi, S. Hasenauer, K. Scipal, H. Bonekamp, J. Figa, and C. Anderson (2007), Initial soil moisture retrievals from the METOP-A Advanced Scatterometer (ASCAT), *Geophys. Res. Lett.*, *34*, L20401, doi:10.1029/2007GL031088.

Boé, J. (2013), Modulation of soil moisture–precipitation interactions over France by large scale circulation, *Clim. Dyn.*, *40*(3-4), 875–892.

Dee, D. P., et al. (2011), The ERA-Interim reanalysis: Configuration and performance of the data assimilation system, *Q. J. R. Meteorol. Soc.*, *137*(656), 553–597.

Dirmeyer, P. A., Y. Jin, B. Singh, and X. Yan (2013), Trends in land–atmosphere interactions from CMIP5 simulations, *J. Hydrometeorol.*, *14*(3), 829–849.

Ek, M. B., and A. A. M. Holtslag (2004), Influence of soil moisture on boundary layer cloud development, *J. Hydrometeorol.*, *5*(1), 86–99.

Eltahir, E. A. B. (1998), A soil moisture-rainfall feedback mechanism 1. Theory and observations, *Water Resour. Res.*, *34*, 765–776, doi:10.1029/97WR03499.

Findell, K. L., and E. A. B. Eltahir (2003), Atmospheric controls on soil moisture-boundary layer interactions. Part I: Framework development, *J. Hydrometeorol.*, *4*(3), 552–569.

Fischer, E. M., S. I. Seneviratne, P. L. Vidale, D. Luthi, and C. Schar (2007), Soil moisture—Atmosphere interactions during the 2003 European summer heat wave, *J. Clim.*, *20*(20), 5081–5099.

Froidevaux, P., L. Schlemmer, J. Schmidli, W. Langhans, and C. Schär (2014), Influence of the background wind on the local soil moisture–precipitation feedback, *J. Atmos. Sci.*, *71*(2), 782–799.

Guo, Z. C., et al. (2006), GLACE: The global land-atmosphere coupling experiment. Part II: Analysis, *J. Hydrometeorol.*, *7*(4), 611–625.

Hauck, C., C. Barthlott, L. Krauss, and N. Kalthoff (2011), Soil moisture variability and its influence on convective precipitation over complex terrain, *Q. J. R. Meteorol. Soc.*, *137*(S1), 42–56.

Haylock, M. R., N. Hofstra, A. Tank, E. J. Klok, P. D. Jones, and M. New (2008), A European daily high-resolution gridded data set of surface temperature and precipitation for 1950–2006, *J. Geophys. Res.*, *113*, D20119, doi:10.1029/2008JD010201.

Hohenegger, C., P. Brockhaus, C. S. Bretherton, and C. Schar (2009), The soil moisture-precipitation feedback in simulations with explicit and parameterized convection, *J. Clim.*, *22*(19), 5003–5020.

Knox, R., G. Bisht, J. Wang, and R. Bras (2011), Precipitation variability over the forest-to-nonforest transition in southwestern Amazonia, *J. Clim.*, *24*(9), 2368–2377.

Koster, R. D., M. J. Suarez, R. W. Higgins, and H. M. Van den Dool (2003), Observational evidence that soil moisture variations affect precipitation, *Geophys. Res. Lett.*, *30*(5), 1241, doi:10.1029/2002GL016571.

Koster, R. D., et al. (2004), Regions of strong coupling between soil moisture and precipitation, *Science*, *305*(5687), 1138–1140.

Koster, R. D., et al. (2010), Contribution of land surface initialization to subseasonal forecast skill: First results from a multi-model experiment, *Geophys. Res. Lett.*, *37*, L02402, doi:10.1029/2009GL041677.

Morel, C., and S. Senesi (2002), A climatology of mesoscale convective systems over Europe using satellite infrared imagery. I: Methodology, *Q. J. R. Meteorol. Soc.*, *128*, 1953–1971.

Pielke, R. A. (2001), Influence of the spatial distribution of vegetation and soils on the prediction of cumulus convective rainfall, *Rev. Geophys.*, *39*(2), 151–177, doi:10.1029/1999RG000072.

Rieck, M., C. Hohenegger, and C. C. van Heerwaarden (2014), The influence of land surface heterogeneities on cloud size development, *Mon. Weather Rev.*, *142*(10), 3830–3846.

Schär, C., D. Lüthi, U. Beyerle, and E. Heise (1999), The soil–precipitation feedback: A process study with a regional climate model, *J. Clim.*, *12*(3), 722–741.

Seneviratne, S. I., et al. (2013), Impact of soil moisture-climate feedbacks on CMIP5 projections: First results from the GLACE-CMIP5 experiment, *Geophys. Res. Lett.*, *40*, 1–6, doi:10.1002/grl.50956.

Taylor, C. M., A. Gounou, F. Guichard, P. P. Harris, R. J. Ellis, F. Couvreux, and M. De Kauwe (2011), Frequency of Sahelian storm initiation enhanced over mesoscale soil-moisture patterns, *Nat. Geosci.*, *4*(7), 430–433.

Taylor, C. M., R. A. M. de Jeu, F. Guichard, P. P. Harris, and W. A. Dorigo (2012), Afternoon rain more likely over drier soils, *Nature*, *489*(7416), 423–426.

Taylor, C. M., C. E. Birch, D. J. Parker, N. Dixon, F. Guichard, G. Nikulin, and G. M. S. Lister (2013), Modeling soil moisture-precipitation feedback in the Sahel: Importance of spatial scale versus convective parameterization, *Geophys. Res. Lett.*, *40*, 6213–6218, doi:10.1002/2013GL058511.

van den Hurk, B., F. Doblas-Reyes, G. Balsamo, R. Koster, S. Seneviratne, and H. Camargo Jr. (2012), Soil moisture effects on seasonal temperature and precipitation forecast scores in Europe, *Clim. Dyn.*, *38*(1–2), 349–362.

van der Ent, R. J., H. H. G. Savenije, B. Schaefli, and S. C. Steele-Dunne (2010), Origin and fate of atmospheric moisture over continents, *Water Resour. Res.*, *46*, W09525, doi:10.1029/2010WR009127.

van Heerwaarden, C. C., J. Vilà-Guerau de Arellano, A. Gounou, F. Guichard, and F. Couvreux (2010), Understanding the daily cycle of evapotranspiration: A method to quantify the influence of forcings and feedbacks, *J. Hydrometeorol.*, *11*(6), 1405–1422.

Zaitchik, B. F., A. K. Macalady, L. R. Bonneau, and R. B. Smith (2006), Europe's 2003 heat wave: A satellite view of impacts and land-atmosphere feedbacks, *Int. J. Climatol.*, *26*(6), 743–769.